Accepted for publication by Applied Acoustics, 9 May 2018, https://doi.org/10.1016/j.apacoust.2018.05.012

Assessment of measurement-based methods for separating wheel and track contributions to railway rolling noise

David Thompson [a*], Giacomo Squicciarini [a], Jin Zhang [a], Ines Lopez Arteaga [b], Elias Zea [b], Michael Dittrich [c], Erwin Jansen [c], Kevin Arcas [d], Ester Cierco [d], Francesc Xavier Magrans [d], Antoine Malkoun [e], Egoitz Iturritxa [f], Ainara Guiral [f], Matthias Stangl [g], Gerald Schleinzer [h], Beatriz Martin Lopez [i], Claire Chaufour [j], Johan Wändell [k]

Affiliations

a. Institute of Sound and Vibration Research, University of Southampton, Southampton SO17 1BJ, UK
b. KTH Royal Institute of Technology, The Marcus Wallenberg Laboratory for Sound and Vibration Research, Teknikringen 8, SE-100 44 Stockholm, Sweden
c. TNO, PO Box 96864, 2509 JG Den Haag, The Netherlands
d. Ingeniería para el Control del Ruido (ICR), C/ Berruguete 52, Vila Olímpica (Vall d'Hebron), 08035 Barcelona, Spain
e. Alstom Transport, 6 rue de Strasbourg, 67110 Reichshoffen, France
f. CAF, Technology Division, R&D Department, J.M. Iturrioz 26, 20200 Beasain, Spain
g. DB Systemtechnik, Völckerstraße 5, 80939 München, Germany
h. Siemens, Eggenberger Straße 31, 8020 Graz, Austria
i. Patentes Talgo S.L., Paseo del Tren Talgo, 2 - E-28290 Las Matas, Madrid, Spain
j. SNCF Innovation & Recherche, Immeuble Lumière, 40, avenue des Terroirs de France, 75611 PARIS Cedex 12, France
k. Bombardier Transportation Acoustic department, Am Rathenaupark, 16761 Hennigsdorf, Germany

*: corresponding author, email: djt@isvr.soton.ac.uk

Abstract

The noise produced during a train pass-by originates from several different sources such as propulsion noise, noise from auxiliary equipment, aerodynamic noise and rolling noise. The rolling noise is radiated by the wheels and the track and is excited by the wheel and rail unevenness, usually referred to as roughness. The current TSI Noise certification method, which must be satisfied by all new mainline trains in Europe, relies on the use of a reference track to quantify the noise from new vehicles. The reference track is defined by an upper limit of the rail roughness and a lower limit of the track decay rate (TDR). However, since neither the rail roughness nor the track radiation can be completely neglected, the result cannot be taken as representing only the vehicle noise and the measurement does not allow separate identification of the noise radiated by wheel and track. It is even likely that further reductions in the limit values for new rolling stock cannot be achieved on current tracks. There is therefore a need for a method to separate the noise into these two components reliably and cheaply. The purpose of the current study is to assess existing and new methods for rolling noise separation. Field tests have been carried out under controlled conditions, allowing the different methods to be compared. The TWINS model is used with measured vibration data to give reference estimates of the wheel and track noise components. Six different methods are then considered that can be used to estimate the track component. It is found that most of these methods can obtain the track component of noise with acceptable accuracy. However, apart from the TWINS model, the wheel noise component could only be estimated directly using three methods and unfortunately these did not give satisfactory results in the current tests.

Keywords: Railway noise; rolling noise; experimental methods; source separation; transfer path analysis; beamforming

1. Introduction

Railway noise originates from several different sources such as propulsion noise, noise from auxiliary equipment, aerodynamic noise at high speeds and rolling noise. The rolling noise is radiated by the vibration of the wheels and the track and is excited by the combined wheel and rail unevenness, usually referred to as roughness [1]. A high level of roughness in combination with low damping of wheel and rail leads to high levels of rolling noise. This noise source is considered to be dominant for train speeds up to more than 300 km/h [2]. In

efforts to reduce rolling noise by improved design and to quantify it in relation to vehicle certification, a key question is related to the separation of the noise radiated by the wheel from that radiated by the track. Without such a separation, certification tests can be influenced by the track properties and do not only measure the vehicle noise. Moreover, improved designs of vehicle or track may not be properly assessed if the vehicle contribution to the noise is masked by the track.

The current certification tests defined in the Technical Specification for Interoperability (TSI) Noise [3] and ISO 3095 [4], which must be satisfied by all new mainline trains in Europe, rely on the use of a reference track to quantify the noise from new vehicles. The reference track is defined by an upper limit of the rail roughness and a lower limit of the track decay rate (TDR) which are intended to minimise the influence of the track on the measurement. However, since neither influence of the rail roughness nor the contribution from the track radiation can be completely neglected in such a test, the result cannot be taken as representing only the vehicle noise and the measurement does not allow separate identification of wheel and track noise contributions.

Current understanding of railway rolling noise is largely based on the theoretical work of Remington [5, 6] and Thompson [1, 7]. This has been implemented in the TWINS model [8], which is a prediction tool, developed on behalf of the European railways (ERRI) in the 1990s. It takes a roughness spectrum as the input and uses the dynamic properties of the wheel (from a finite element model) and the track (from an analytical model) to calculate their dynamic interaction. Sound radiation is calculated from the vibration of wheel, rail and sleeper. Validation measurements [8, 9, 10] have shown that the model can predict the overall noise level to within ±2 dB and the result in any one-third octave band to within about ±5 dB. However, this uncertainty was largely attributed to uncertainty in the inputs, particularly the roughness. The division into wheel and track components was also verified by means of intermediate vibration measurements. The estimates of radiated sound due to wheel and track vibration were found to be reliable to within about ±2 dB in any one-third octave band provided that wheel and rail vibration measurements are available. Although TWINS can be considered to be an accurate separation method, the emphasis in the present work is on developing a method that is experimentally based and therefore less reliant on expertise in

using the models. Moreover, it should not require measurements on the vehicle such as wheel vibration but should be possible to execute from the trackside.

The roughness of the wheels and rails can be measured directly [11, 12]. For the TSI and ISO test procedure [3, 4] it is required to measure the rail roughness of the test site. However, measurements of wheel roughness are not required and would add considerable extra effort. An alternative is provided by the Pass-by Analysis method (PBA) which uses rail vibration measurements to extract the track decay rate, the combined effective roughness and the total transfer function from roughness to noise [13, 14, 15]. The PBA method does not directly separate wheel and track contributions although it can form the basis for separation methods, as described later in this paper.

Several experimental methods for performing this separation have been proposed and tested in previous work with varying results. Different levels of rolling noise separation were defined within the STAIRRS project [13]. Level 0 indicates that no separation is achieved; only overall noise levels are obtained. Level 1 separation provides the wheel and track sound pressure levels in a given situation. Level 2 separation provides the wheel and rail roughness as well as the vehicle and track transfer functions. Level 3 separation is intended to provide all necessary data to assess the complete vehicle and track interactions. This would normally only be required if the vehicle or track are non-standard, for example with resilient wheels.

Various types of acoustic transfer functions can be determined for the track and the vehicle separately by using measurements on a stationary vehicle and track. In particular, transfer functions from contact force to sound pressure can be measured directly using an instrumented hammer impacting on the wheel or rail surface or reciprocally by using a loudspeaker near the track [16]. The latter is preferred as it can overcome potential problems of poor coherence in direct measurements using an impact hammer. For the track transfer function, ideally the vehicle should be present but dynamically decoupled from the track, which is difficult to achieve. For the wheel measurement the vehicle should again be decoupled from the track but some artificial damping should be introduced to simulate the ‘rolling damping’ present during running. In order to use these transfer functions to obtain the vehicle and track noise contributions from a moving vehicle, they have to be converted into transfer functions from combined roughness to sound pressure. To achieve this some correction functions were derived in the STAIRRS project based on the TWINS model [13].

The results are used with measurements of the combined wheel and rail roughness to determine the track and vehicle contributions to the rolling noise.

Another method developed in the STAIRRS project is called the MISO method (Multiple Input Single Output separation method) [17]. This was based on simultaneous measurements of the sound pressure and track vibration during the train pass-by. The vibroacoustic Frequency Response Functions (FRFs) between the track vibration signals and the sound pressure at a close microphone were determined using the parts of the signals corresponding to the middle of the vehicles. These were combined with the vibration measured over the whole pass-by to estimate the track contribution. The result could then be transposed to the standard microphone position using geometrical attenuation.

A ‘reference vehicle’ method was proposed and tested in the METARAIL project [18, 19] and further investigated in the STAIRRS project [13]. The principle was to measure the sound pressure level and rail vertical vibration level during the passage of a quiet vehicle with only rolling noise sources and relatively quiet wheels. These measurements were used to estimate a transfer function for the track by assuming that the vehicle contribution is negligible. The test vehicle was then measured in the same way. The track contribution was determined from the rail vibration during the passage of the test vehicle and the previously determined track transfer function. Some experience was gained with this method using wagons with bogie-mounted shields [18]. These reference vehicles were not ideal, however, as the shielding also reduced the track noise contribution. Vehicles with small wheels were used in reference [13].

In a similar way, the use of a reference track method could be envisaged to determine the vehicle contribution. However, even for a quiet TSI-compliant track, the track contribution usually exceeds the vehicle one over a large part of the frequency range. No current track design is known that would be suitable for such a method.

Microphone arrays with beamforming [20] have been used since the 1980s to locate sources on a moving train, with the main application being aerodynamic sources [21, 22]. The steering of the array should follow the moving source and the Doppler shift should be removed from the signals, for example by resampling [23]. The spatial resolution depends on the frequency, with the width (aperture) of the main lobe in the array pattern depending on

the ratio of the acoustic wavelength to the array size. Thus at low frequencies large arrays are required and it becomes difficult to separate sources that are close together. Conversely at high frequencies the results can be subject to spatial aliasing leading to ghost images.

Some attempts have been made to use microphone arrays to study rolling noise [24, 25]. However, a common feature of these measurements is that the wheel noise is found to be prominent. Although this may be the case in the situations considered, Kitagawa and Thompson [26] indicated that the assumption of a distribution of uncorrelated point sources in beamforming processing is not appropriate for the rail, which is a distributed source radiating at a certain angle with respect to the normal. If the array is focused mainly in a direction normal to the rail it is expected that this will suppress the rail contribution [26]. This is considered in the present paper as the basis of a new method to identify the wheel contribution.

The purpose of the study presented here is to assess existing and new methods for rolling noise separation. Dedicated field tests have been carried out under controlled conditions allowing the different methods to be compared. The principle of wheel and track separation is summarised in Section 2 and the field measurements are described in Section 3. The TWINS model [8] is used with measured vibration data to give reference estimates of the wheel and rail contributions as described in Section 4. Six different methods are then introduced in Section 5 that can be used to estimate the track component and three that can estimate the vehicle component (two of which are common to the assessment of both track and vehicle components). Each has been applied independently by different organisations and the results have been compared with the reference results without further adjustment or tuning. A comparison of the results is presented in Section 6 and conclusions are given in Section 7.

2. Overview of noise sources

Figure 1 shows schematically the various sources contributing to the noise during a train pass-by. The purpose of a separation method is to identify the different contributions to the measured noise. The noise emission is defined over the transit time T_p of the train (or vehicle) pass-by at constant speed, as used in the TSI [3] and ISO standard [4]. The pass-by sound pressure level is obtained in the form $L_{p\mathrm{Aeq,Tp}}$ measured at 7.5 m from the track centreline and 1.2 m above the top of rail.

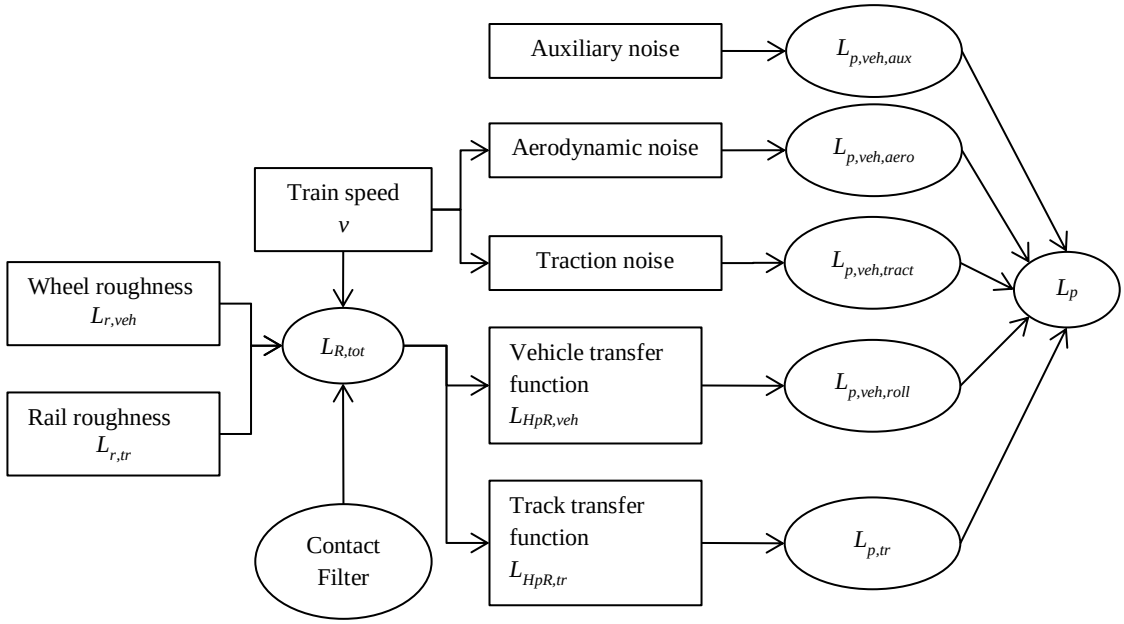

Figure 1. Schematic representation of the vehicle and track contributions including rolling noise and other sources, and excitation by wheel and rail roughness and vehicle and track transfer functions.

The pass-by sound pressure level in dB can be expressed as the energy sum (i.e. the sum of mean square pressures given in dB, symbol ⊕) of the noise radiated by the vehicle $L_{p,\mathrm{veh}}$ and by the track $L_{p,\mathrm{tr}}$ (omitting the subscripts Aeq,Tp for clarity):

$$L_p(v, f) = L_{p,\mathrm{tr}} \oplus L_{p,\mathrm{veh}} \tag{1}$$

The vehicle noise can be expressed as the energy sum of rolling noise $L_{p,\mathrm{veh,roll}}$, traction noise $L_{p,\mathrm{veh,tract}}$, aerodynamic noise $L_{p,\mathrm{veh,aero}}$ and noise from auxiliary systems such as ventilation fans $L_{p,\mathrm{veh,aux}}$:

$$L_{p,\mathrm{veh}} = L_{p,\mathrm{veh,roll}} \oplus L_{p,\mathrm{veh,tract}} \oplus L_{p,\mathrm{veh,aero}} \oplus L_{p,\mathrm{veh,aux}} \tag{2}$$

In this paper, only rolling noise sources are considered, so the separation methods under consideration are limited to those identifying wheel and/or track rolling noise contributions.

If other sources such as motors, fans or aerodynamic noise can be neglected, equation (1) applies but with both components consisting only of rolling noise. This corresponds to Level 1 separation [13].

The representation of rolling noise in Figure 1 is based on the TWINS model [8]. The rolling noise is excited by the combination of wheel and rail roughness. The total effective roughness level in dB $L_{R,\mathrm{tot}}$ in a particular frequency band is given by the energy sum of the rail roughness $L_{r,\mathrm{tr}}$ and the wheel roughness $L_{r,\mathrm{veh}}$, modified by the contact filter CF, expressed in dB [15]:

$$L_{R,\mathrm{tot}} = \left(L_{r,\mathrm{tr}} \oplus L_{r,\mathrm{veh}}\right) + \mathrm{CF} \tag{3}$$

The roughness is a function of wavelength λ so that the corresponding frequencies f depend on the train speed v according to:

$$f = v / \lambda \tag{4}$$

The total effective roughness excites both the wheel and the track, causing them both to radiate noise. Thus the vehicle noise can be expressed as a combination of the total effective roughness level and a transfer function $L_{HpR,\mathrm{veh}}$ from effective roughness to sound pressure, also expressed in dB:

$$L_{p,\mathrm{veh}} = L_{R,\mathrm{tot}} + L_{HpR,\mathrm{veh}} \tag{5}$$

where, in this case, the addition is a simple arithmetic addition of dB values. Similarly, the track noise can be expressed as a combination of the total effective roughness level and a transfer function $L_{HpR,\mathrm{tr}}$:

$$L_{p,\mathrm{tr}} = L_{R,\mathrm{tot}} + L_{HpR,\mathrm{tr}} \tag{6}$$

These transfer functions can also be normalised to the number of axles per unit length, $APL = N_{\mathrm{ax}}/L_{\mathrm{veh}}$ where N_{ax} is the number of axles per vehicle and L_{veh} is the vehicle length [13]. This

normalisation is required if track transfer functions are to be compared between different vehicle types.

As the TSI requires only the overall A-weighted level it would be sufficient in the first instance to provide Level 1 separation in terms of overall levels. However, to provide more information, separation in terms of one-third octave spectra is preferred. Moreover, Level 2 separation allows results to be transferred to other situations, for example other speeds, or even other sites. An intermediate level ("Level 1.5") could be envisaged where the vehicle and track transfer functions are obtained but only the total roughness is known, not separated into wheel and rail.

It should be mentioned that the vehicle contribution can, in principle, be estimated from the total and track noise levels by using a subtraction:

$$L_{p,\mathrm{veh}} = 10\log_{10}\left(10^{L_{p,\mathrm{tot}}/10} - 10^{L_{p,\mathrm{tr}}/10}\right) \tag{7}$$

However, care must be taken when using this formula, especially when the vehicle noise level is similar to or less than the track noise level, as the uncertainty can be increased considerably by the subtraction operation. As an example, Figure 2 shows half the error range in the wheel noise estimate introduced by an error margin of ±1, ±1.5 and ±2 dB in the track noise estimate (assuming that the total noise is determined correctly). This is plotted against $L_{p,\mathrm{tot}} - L_{p,\mathrm{tr}}$, the level difference between total noise and track noise. If the track noise contribution is 3 dB less than the total, indicating that wheel and track contributions are equal, the error in the wheel noise estimate is greater than that in the track noise. If the level difference is smaller than 3 dB the error in the wheel noise estimate increases dramatically. If uncertainties are also present in the total noise the error margins increase further. For this reason, methods relying on Equation (7) are not considered in the present study.

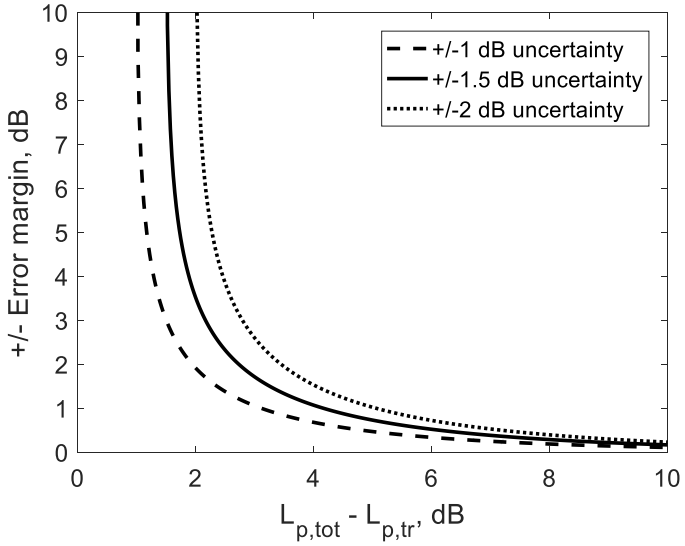

Figure 2. Half the error range in wheel noise estimate from Eq. (7) assuming that the total noise is known correctly and that the track noise has an uncertainty of ±1, ±1.5 or ±2 dB.

3. Measurement campaign

A measurement campaign was arranged to collect data to test various separation methods. A dedicated test train was used for the measurements consisting of an electric locomotive and three similar carriages, as shown in Figure 3. The carriage wheels were of type BA093 with diameter, as new, of 0.95 m. The wheels on the test bogie had a partially worn diameter of 0.938 m. The vehicles were all disc-braked to give smooth wheels. On the central carriage, one bogie, used as the test bogie, was unbraked to ensure that the roughness remained the same. Apart from the locomotive, the only sources of noise on the train were from rolling noise (wheels and track). By analysing the sound spectra from different parts of the train it was found that the noise levels when the locomotive was in front of the microphones were up to 10-15 dB higher than the rest of the train for frequencies below 630 Hz. However, there were no consistent differences between the results for bogies 4/5, 6/7 and 8, confirming that the locomotive had negligible influence on the results at the centre and rear of the train.

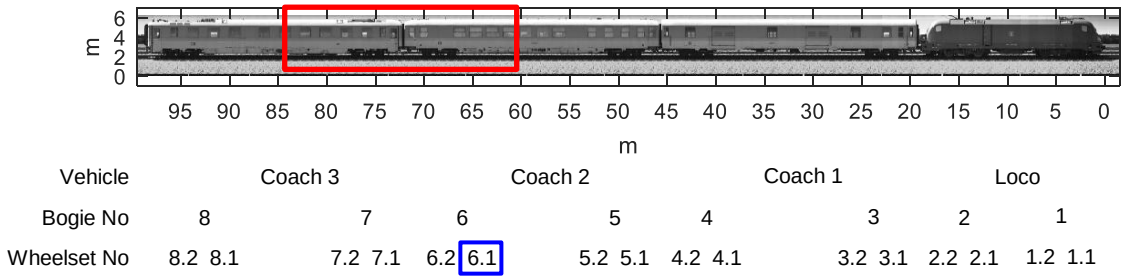

Figure 3. Schematic view of test train indicating the test wheelset (6.1). The red rectangle indicates the test section used for analysis.

One wheel (numbered 6.1 in Figure 3) was instrumented with accelerometers and a telemetry system to allow the vibration of the wheel to be measured during the train passages. A telemetry system was used to transmit the acceleration signals to recording equipment inside the vehicle. A similar procedure was used for example in [8]. The mobilities of this wheel in axial and radial directions were measured prior to the running tests and used to tune a finite element model of the wheel by adjusting the natural frequencies and modal damping ratios. The measured and calculated mobilities are shown in Figure 4.

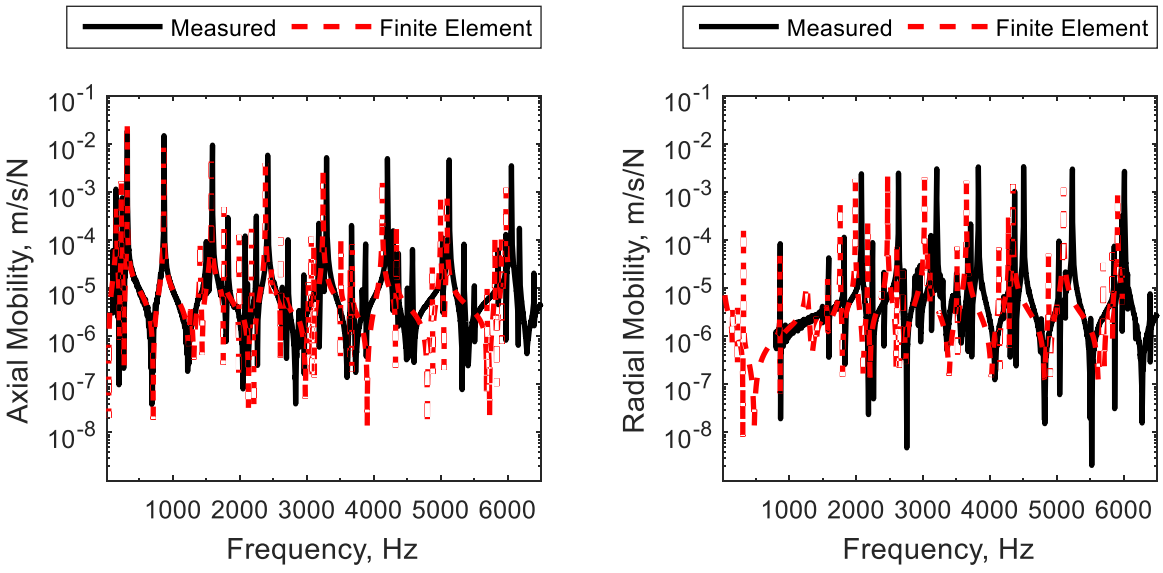

(a) (b)

Figure 4. Wheel point mobilities: (a) axial; (b) radial.

The test site was located near Haspelmoor, north of Munich in Germany. The track consisted of UIC60 rails mounted with relatively soft rail pads on concrete monoblock sleepers laid in ballast. The track at the test section was straight and free of gradient. The track decay rates

for vertical and lateral motion were measured in accordance with EN 15461 [27], and are shown in Figure 5. These decay rates are rather low in comparison with the limits given in the TSI [3]. By fitting these measurements with results from a track vibration model based on a Timoshenko beam on a dual layer foundation [1], the dynamic pad stiffness was identified as 105 MN/m in the vertical direction and 14 MN/m in the lateral direction. The results from the model are also shown in Figure 5 for comparison.

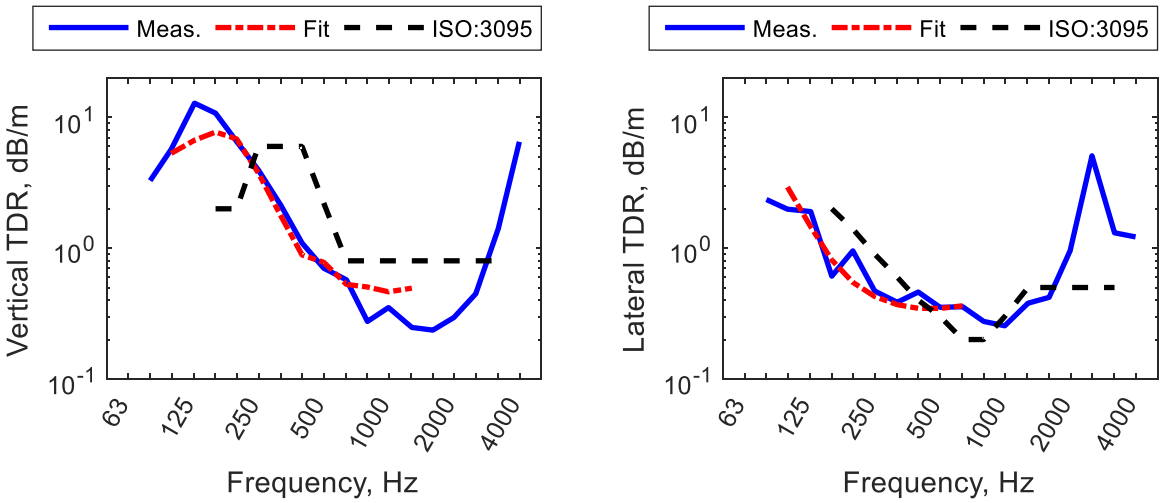

(a) (b)

Figure 5. Track decay rates (a) vertical; (b) lateral.

The rail roughness was measured using a corrugation analysis trolley [11] and analysed into one-third octave bands of wavelength. The average spectrum is shown in Figure 6 and compared with the limit curve from ISO 3095:2013 [4] from which it can be seen that the track was relatively smooth although slightly above the limit between 20 and 40 mm wavelength.

The wheel roughness of the four wheels in the test bogie was measured using the system RM1435. Three traces were measured on each wheel, at the nominal running line and at ±10 mm. The average of these measurements over all four wheels is shown in Figure 6. The wheels can be seen to be smoother than the rails apart from the wavelength range between 0.1 and 0.315 m. Considerable variation was found in the roughness between different wheels at wavelengths longer than about 50 mm.

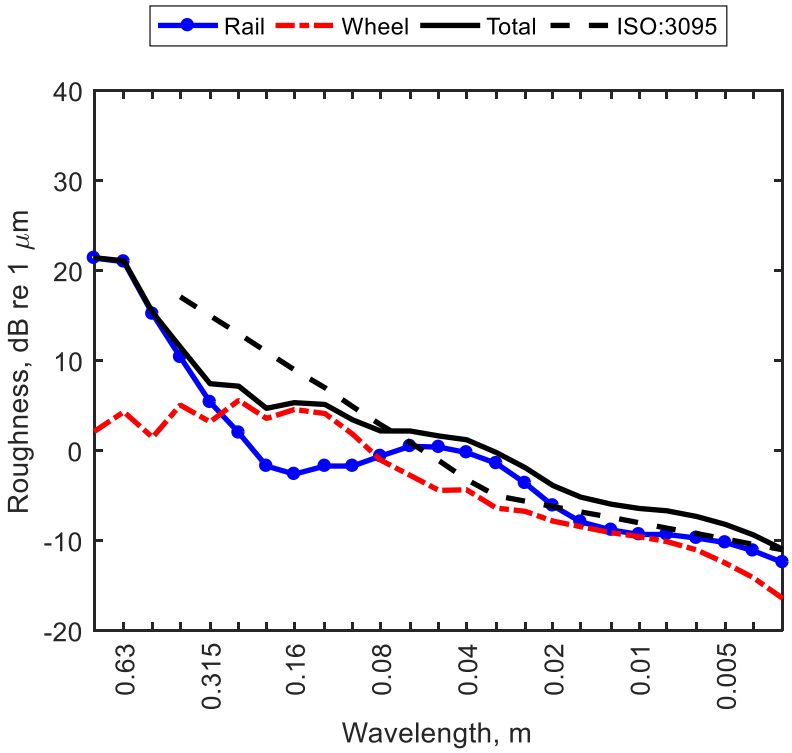

Figure 6. Average rail and wheel roughness spectra and total roughness.

The track was instrumented at three different contiguous sections with accelerometers and microphones for use with the different separation methods described below. Different microphone positions were used at the three sections, as listed in Table 1, which also indicates the separation methods tested at each section. Details of these methods and the instrumentation used will be given in the appropriate sections of the paper.

It was confirmed that the track decay rates and rail roughness were similar at each of these track sections. The test train ran past the trackside instrumentation a number of times over a period of two days in June 2016, giving results for three runs at each of 40, 80 and 160 km/h. The locomotive, although not coasting, was driven on minimum power to maintain a constant speed. During the test runs the train always passed in the same direction.

Table 1. Details of the measurement sections used for each method

Method	Track section	Microphone distance from nearest rail (m)	Microphone height above rail head (m)
Beamforming TWINS with track vibration PBA with assumed distribution function PBA with previous vehicle transfer function	A	7.5	1.5
Wave Signature Extraction (WSE)	B	1.2	–0.1
Advanced Transfer Path Analysis (ATPA) MISO method	C	2.8	0.5

4. Reference results

For comparison with the results obtained with the various separation methods tested in this study, a set of 'reference' results has been produced for each track section; different noise levels are obtained at each section due to the different microphone positions, as listed in Table 1. To obtain these reference results, use is made of the TWINS model [8] together with measured vibration data.

The TWINS model can be used to predict the various components of radiated noise and has been validated through field measurements [8, 9, 10]. It is normally used with inputs consisting of measured wheel and rail roughness and various parameters to define the track and wheel dynamic properties. However, to improve the reliability of the separation achieved, in the present study it is used with measured vibration. In [10] it is shown that the uncertainty in the predictions is much reduced by basing them on measured vibration.

Poor agreement with measured noise was obtained below 315 Hz, but this is possibly due to the influence of wind on the microphones, especially at the close positions. In the analysis only the results from 315 Hz to 5000 Hz have been used, which are sufficient to determine the overall A-weighted levels to within 0.2 dB compared with the full spectrum.

The procedure followed was that first a TWINS model was produced using best estimates of various parameters, including rail pad stiffness, track decay rates and wheel mobilities. The resulting predicted spectra were found to be close to the measured ones although with some differences. It is not possible to enter measured vibration directly into the TWINS software. Therefore, to obtain an estimate of the track noise corresponding to the measured track vibration, the predicted levels of track noise were adjusted by multiplying by the ratio of measured to predicted track vibration. This was carried out separately for the rail vertical, rail lateral and sleeper contributions. The measured wheel vibration has not been used in this step as this was found to lead to worse agreement with the overall noise; instead, the predicted wheel noise from the previous step is retained. Nevertheless, the predicted wheel vibration spectra have been checked against the measured ones and found to be broadly consistent, as shown in Figure 7. Differences may have occurred due to uncertainties in locating the exact section of the pass-by corresponding to the test section. Moreover, the measured vibration represents a single wheel whereas the TWINS prediction should represent all wheels in the test section and therefore uses the average roughness.

Finally a small difference remained with the measured noise spectrum, so all components were adjusted such that the total noise matched the measured noise spectra; that is, the difference between measured and predicted total noise is applied as a correction to each component. It is assumed, in performing this step, that the measured noise consists only of rolling noise, and that the relative contributions of wheel and track in the prediction are correct in each frequency band. The corrections applied in the final step, i.e. the differences between the total predicted noise and the measured noise, are shown in Figure 8. These differences are mostly less than 2 dB with a standard deviation of 1.5 dB and a maximum value of 4.1 dB.

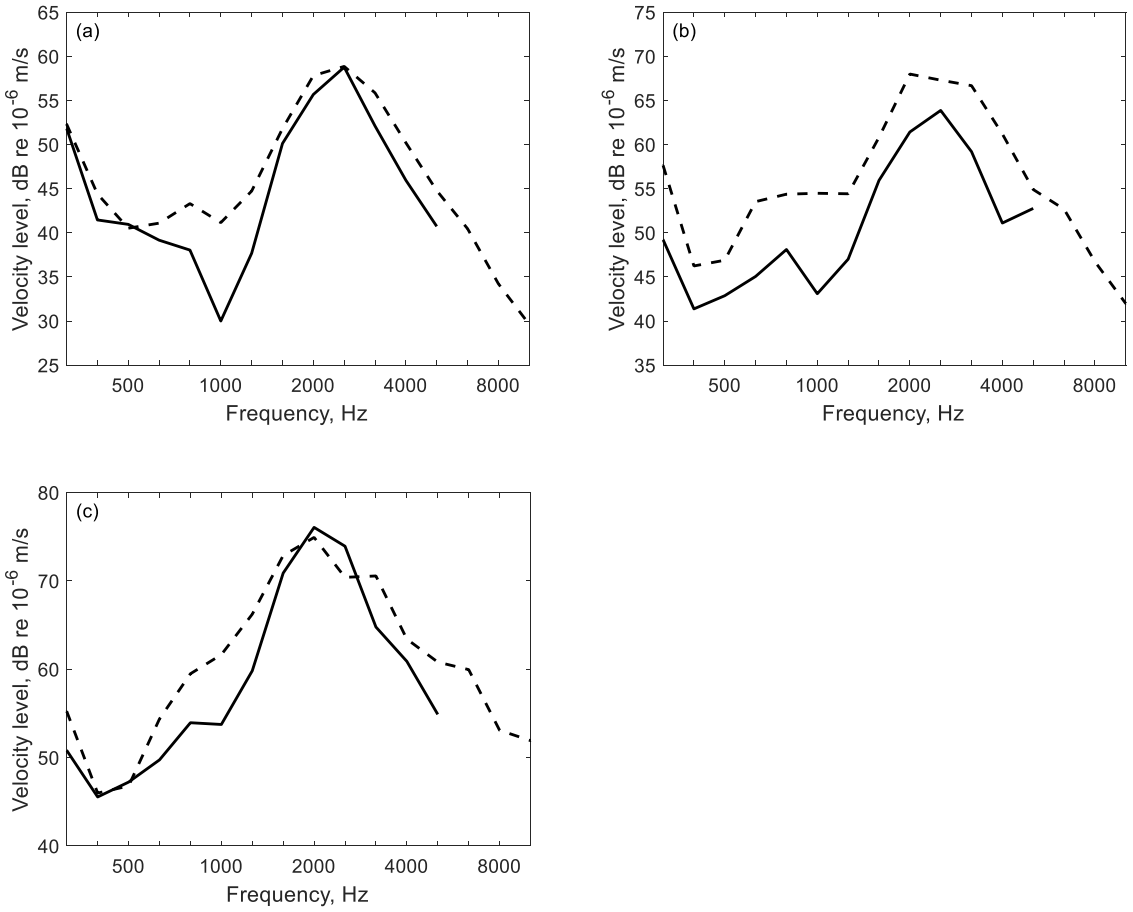

Figure 7. Comparison of measured axial wheel vibration with results from TWINS for three runs. (a) 40 km/h; (b) 80 km/h; (c) 160 km/h. - - - Measured, — calculated.

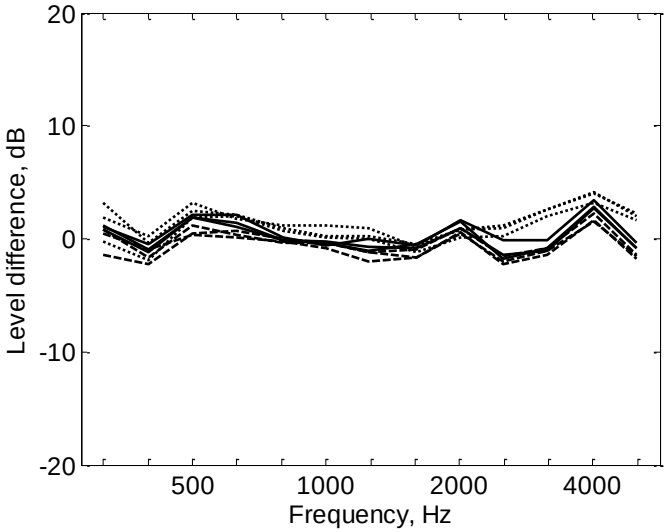

Figure 8. Corrections applied to the reference results in the final step of the procedure. - - - 40 km/h, — 80 km/h, ····· 160 km/h.

Figure 9 shows an example of the contributions of wheel, rail vertical, rail lateral and sleeper vibration to the overall noise spectrum at track section A after applying the adjustments described above. Characteristically, the wheel is the dominant component above 2 kHz whereas the rail is dominant between 315 and 1600 Hz, with the vertical component of rail noise greater than the lateral above 630 Hz and the lateral component greater below this frequency. The wheel is also important at 250 Hz. Similar results have been found previously for other wheel and track designs [9, 10].

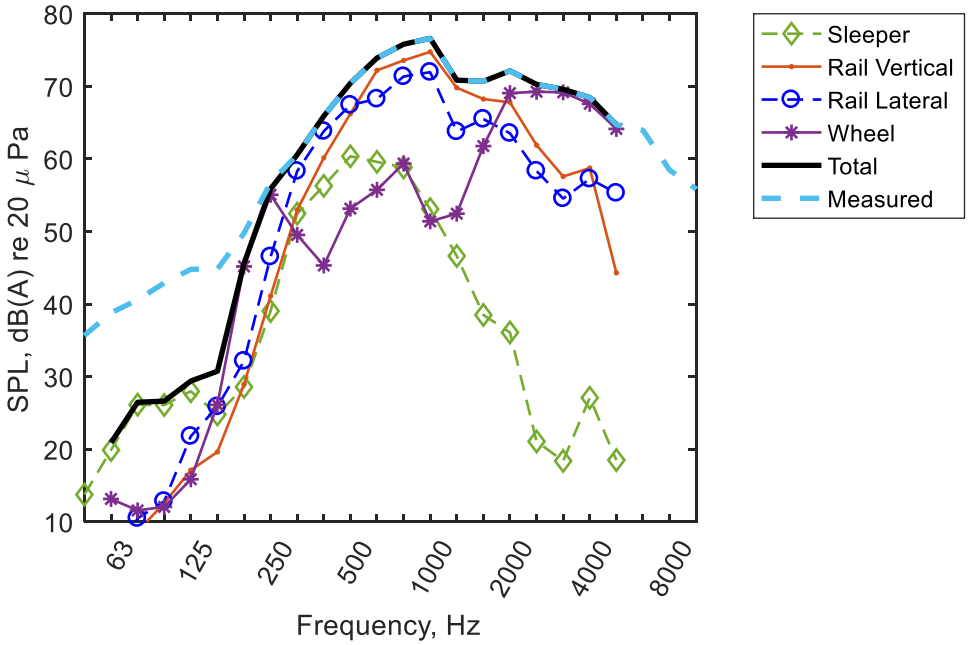

Figure 9. Reference separation based on TWINS results after adjustment to match total measured spectrum at track section A. Example run at 80 km/h, shown as A-weighted spectra.

The measured overall noise levels at track section A, together with the track and wheel components according to the reference results, are listed in Table 2. These are expressed as $L_{pAeq,Tp}$ averaged over the length of the test section marked in Figure 3. From this it can be seen that the track contribution is within 0.9 to 1.7 dB of the total noise, suggesting that estimates of the wheel noise based on Equation (7) would be subject to very large uncertainty, see Figure 2. According to the results in Table 2 the noise levels from the track are between 3.2 and 6.4 dB greater than those from the wheel. Similar trends are found for the other track sections.

The method used to obtain these reference results is not considered as a practical method of separation, since it is not expected that all the data required for this analysis would normally be available as part of a TSI test, in particular the tuned wheel model, wheel roughness and wheel vibration (although the latter was not used here). However, the results obtained here should provide a good approximation to the actual separation between wheel and track noise components and are therefore considered as reference results.

Table 2. Summary of A-weighted noise levels obtained according to reference results for track section A, $L_{pAeq,Tp}$ dB re 2×10^{-5} Pa (based on 315 Hz to 5000 Hz one-third octave bands)

	Total	Track	Wheel
40 km/h	73.4	71.7	68.5
80 km/h	82.9	82.0	75.6
160 km/h	91.9	90.4	86.7

5. Separation methods

5.1. Wave signature extraction

A new method based on wave signature extraction (WSE) using a near-field microphone array has been developed as part of this work. Further details are given in Zea et al. [28, 29]. The method has some similarities to the SWEAM method [30]. The main idea of WSE is to estimate the track contribution by means of wavenumber-domain filters, which are designed according to the radiation properties of the rail. In the frequency region where waves propagate in the rail, it acts as a distributed source with plane wave (or more correctly cylindrical wave) radiation [26]. The angle of the wave-front with respect to the rail can be identified in the wavenumber spectra of the array data, and this can be filtered in order to separate the rail contribution from all other sources. Furthermore, since the rail radiates sound both before and after the train passes the array, the wavenumber filter pass-band (corresponding to the sound field radiated by the rail bending waves) can be found from the dispersion curve obtained from measurement data before and after the pass-by. This avoids any need to characterise the wave motion in the track by static tests prior to the pass-by measurement.

A linear array of 42 equally-spaced microphones was located at 1.2 m from the nearest rail at the same height as the centre of the rail web in track section B, as shown in Figure 10. The microphone spacing was 0.08 m, which is sufficient to identify waves present in the rail for frequencies up to 2 kHz. The temporal sampling frequency was therefore limited, allowing analysis only up to the 2 kHz one-third octave band. Two accelerometers were located on the track and used as reference sensors.

Figure 10. Photograph of the linear microphone array setup at the WSE site.

5.2. Beamforming

A method was proposed using beamforming for wheel/rail source separation, which relies on the fact that the radiation from the rail mainly occurs at an angle to the normal that is at least 10° [26]. Thus by restricting the focus angle of the array within a narrow range, ±10° to the normal, the sound radiation from waves propagating along the rail should be suppressed and only the radiation from the wheel should remain. Additionally there will be a small contribution from the sleepers and the near-field vibration of the rail close to each wheel.

The microphone array adopted for the tests is shown in Figure 11. It was equipped with 72 microphones arranged over nine spirals. The distances between the microphones decreased towards the centre of the array to allow better results to be obtained at high frequencies while

the outer microphones were arranged over a 4 m diameter circle to allow localisation of sources at low frequencies. During the pass by tests, the microphone array was mounted at track section A at 7.5 m from the nearest rail (8.25 m from the track centre), and the centre of the array was at 1.51 m above the top of the railhead. The frequency range over which results can be obtained is 500 Hz to 5000 Hz. The main lobe of the array pattern increases in size as the frequency is reduced; at 500 Hz it already has a diameter of 2.6 m (at the 3 dB-down point) for this microphone configuration.

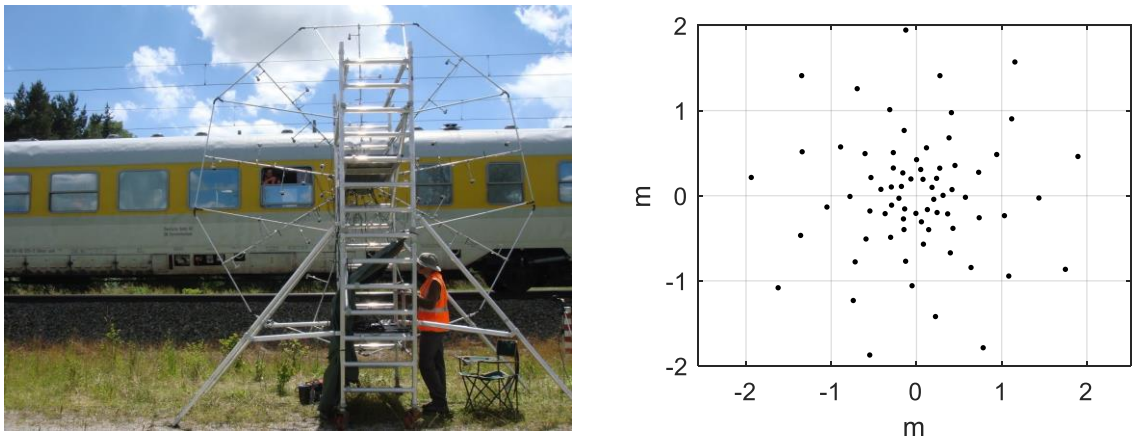

(a) (b)

Figure 11. (a) Microphone array used for beamforming; (b) microphone positions in the array.

The output from the array is processed by first removing the Doppler shift according to different focus points on the train. Then, frequency spectra are taken for a scanning length corresponding to a ±10° viewing angle. A frequency domain beamforming approach for moving sources is then adopted. This makes use of a weighting function based on a linearized approximation for the source motion. More details on the procedure adopted can be found in [31]. This results in overlapping beamforming maps which are averaged. The energy within the map in each one-third octave band is integrated over a rectangular region surrounding each bogie. A frequency-dependent compensation is applied to obtain results that correspond to the sound pressure spectrum at the centre of the array. To calculate this compensation a beamforming map is first obtained from simulations of a moving monopole source using the same method. The spectrum for the moving monopole is obtained by integrating the beamforming map over a rectangular area of the same dimension as that used for the bogie; the compensation is finally calculated from the difference between the beamforming

spectrum and the sound pressure spectrum of a single microphone located at the array centre. The result of this analysis is assumed to be the wheel contribution. A small contribution from the near-field vibration of the rail and the sleepers will also be captured but this is expected to be negligible compared with the radiation from propagating waves in the rail.

An example of the beamforming map is given in Figure 12. The vertical coordinate of 0 m corresponds to the top of the rail. The rectangular integration regions are also shown; these have dimensions 5.0 × 2.4 m. Figure 12(b) shows the overall results for the full frequency range considered, 500 to 5000 Hz, whereas Figure 12(c) shows the results for the high frequency region, 1250 to 5000 Hz, where the wheel component is expected to be dominant. From these results, especially Figure 12(b), it is clear that the beamforming analysis has not completely suppressed the rail noise component in the current configuration.

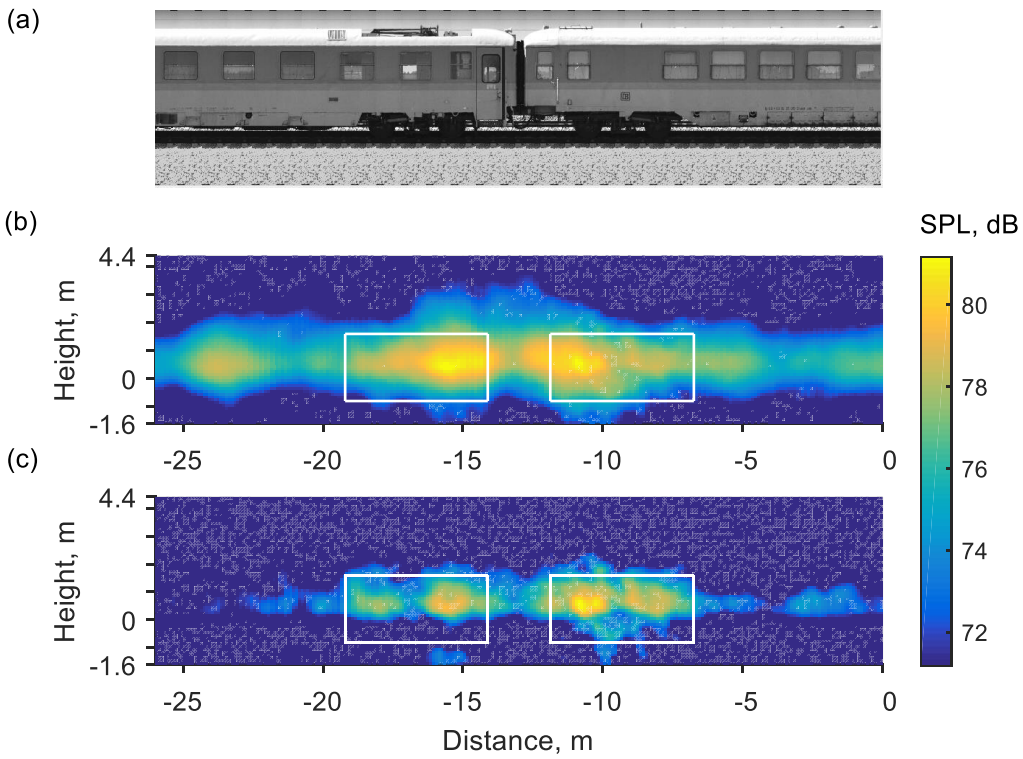

Figure 12. Example of beamforming results. (a) Outline of the test train; (b) overall map for 500 to 5000 Hz; (c) overall map for 1250 to 5000 Hz. Range of colourmap is 10 dB. White boxes indicate region around bogies that are integrated to give source power.

5.3. TWINS model with measured track vibration

As a complementary method to estimate the track contribution, measured track vibration is used with the radiation models from TWINS. The vibration of the track was measured at the same section as the beamforming method during train pass-bys by three accelerometers. These measured the lateral direction in the centre of the rail web (above a sleeper), the vertical direction beneath the centre of the rail foot (adjacent to a sleeper) and the vertical sleeper vibration near the end of the sleeper. The accelerometers were located directly in front of the centre of the microphone array. These signals are used with the radiation models from TWINS to estimate the track contribution. This corresponds to the second step of the reference method, i.e. before adjustment of the overall spectrum, see Section 4. This method can be used to determine the track noise component independently of the beamforming method.

5.4. Advanced transfer path analysis

The Advanced Transfer Path Analysis (ATPA) method is an experimental method for obtaining the noise contributions from the different parts of a system [32]. The objective of the method is to obtain the decomposition of the sound pressure P_M at a target location M as the sum of N noise contributions.

In a system with N subsystems, the ATPA method performs the following decomposition of the total noise P_M at time t_j [32]:

$$p_M(\omega, t_j) = \sum_{k=1}^{N} a_k(\omega, t_j) \cdot T^D_{k \to M}(\omega, t_j) \tag{8}$$

where $a_k(\omega, t_j) \cdot T^D_{k \to M}(\omega, t_j)$ is the contribution of each subsystem k to the total noise. This contribution is obtained as the product of the vibration signal during the train pass-by a_k with the so-called Direct Transfer Function (DTF) $T^D{}_{k \to M}$ from subsystem k to noise at the target location M, which describes the noise produced at M by the vibration of the subsystem k when all other subsystems are blocked (forced to have zero acceleration). There is no requirement for the signals to be correlated.

The so-called ‘Global Transfer Functions’ (GTF) correspond to the physical transfer functions measured when performing impact testing with excitation at one subsystem. Both DTFs and GTFs are characteristics of the physical system and do not depend on operating conditions. However, GTFs can be measured experimentally, but not DTFs. GTFs and DTFs are mathematically related as follows [32]:

$$\begin{pmatrix} \hat{T}_{11}^{G} & \cdots & \hat{T}_{1n}^{G} \\ \vdots & \ddots & \vdots \\ \hat{T}_{n1}^{G} & \cdots & \hat{T}_{nn}^{G} \end{pmatrix} \cdot \begin{pmatrix} -1 & \cdots & \hat{T}_{1n}^{D} \\ \vdots & \ddots & \vdots \\ \hat{T}_{n1}^{D} & \cdots & -1 \end{pmatrix} = \begin{pmatrix} -\hat{T}_{11}^{D} & \cdots & 0 \\ \vdots & \ddots & \vdots \\ 0 & \cdots & -\hat{T}_{nn}^{D} \end{pmatrix} \tag{9}$$

In the application of ATPA, the measurement process is divided in two main phases: the static tests and the running tests. In the static tests, impact testing is used to measure the GTFs and the data are post-processed to obtain the DTFs. The vibration of each subsystem a_k is then measured during train passages. The contributions of each subsystem can be obtained as the product of these signals from the running tests with the DTFs obtained previously, see Equation (8). Some preliminary static tests were presented in [33] to apply the method to the rolling noise separation problem.

The instrumentation used in the measurements is shown in Figure 13. A microphone (M3) was located in front of the instrumented track section at a distance of 3.55 m from the track centreline and a height of 0.5 m above the rail head. The distance of 3.55 m was chosen to ensure that the instrumented length would be sufficient: a longer instrumented length would be required if the TSI position at 7.5 m was used.

The track at section C was separated into six contiguous regions with a spacing of twice the distance between sleepers (1.2 m), leading to a total instrumented section length of 7.2 m. For each region, five accelerometers were installed: one vertical and one lateral accelerometer on each rail and one vertical accelerometer at the centre of the sleeper. The global transfer functions were obtained by exciting each track section using a simple hammer (it is not required to measure the force) and measuring the transfer functions between the acceleration of all sections and the sound pressure at the target microphone M3. The impact loads were applied to both rails and to the sleepers. For frequencies between 50 Hz and 2 kHz the

coherence was good enough to use conventional transfer functions, whereas at high frequencies energetic transfer functions were used. To allow for the effects of the presence of the train on the vibration paths and on the acoustic propagation paths, the transfer functions have been measured with the presence of the train on the track. Additionally, during the static tests with the train on the track, eight accelerometers were mounted on the train, with two on each of the four wheels of the bogie present on the instrumented track section. These accelerometers on the wheels were installed in order to obtain DTFs from the track subsystems without the contribution from the wheel radiation.

Some simplifications of the ATPA procedure have also been investigated in which a more limited set of transducers is used [34]. The aim of these simplifications is to reduce the number of sensors required for application of the ATPA method. The results were favourable, but they are not presented here.

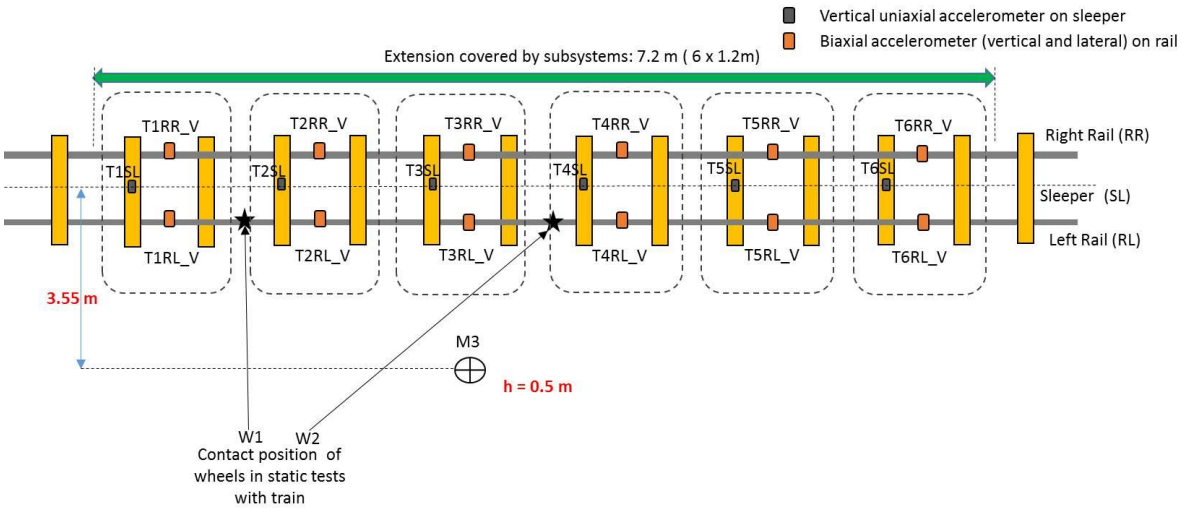

Figure 13. Scheme of instrumentation of the track for static tests.

5.5. MISO method

The MISO method [17] was added to the comparison at a late stage and so has been applied using the instrumentation intended for the ATPA method. Instrumentation at a single cross-section is used, with vertical and lateral accelerometers on each rail, and a single accelerometer on the sleeper. In the original implementation in [17], a microphone at a close position (1.75 m from the track centre) and another at the standard position at 7.5 m were

used. A trigger was used to locate the train wheels in the recorded signals and a time delay correction was applied to the microphone signals in order to take into account the sound propagation speed. In the present implementation, as no trigger was available, a trigger was reconstructed from the rail vibration.

The vibroacoustic Frequency Response Functions (FRFs) between the track vibration signals and the sound pressure at the close microphone are determined using the parts of the signals corresponding to the middle of the vehicles, which are assumed to be free of vehicle contribution. These are combined with the vibration measured over the whole pass-by to estimate the track noise contribution, assuming that the FRFs are the same at the bogie regions as in the vehicle centre. Principal component analysis is used to select the number of independent signals to be used from the five track transducers [17].

The microphone position in track section C is at 3.55 m from the track centre, which is further away than intended in the original implementation of the method (1.75 m). This means that the estimate of track noise obtained from the centre of the train may have been contaminated to some extent by noise from the bogie regions. Finally the results are expressed in terms of the sound pressure levels at 3.55 m as the results at 7.5 m were not available at this track section.

5.6. Methods based on pass-by analysis (PBA)

The pass-by analysis (PBA) method [13] uses measured rail vibration to determine the track decay rate and combined effective roughness. The track decay rate is determined by averaging the rail vibration over short lengths around each wheel and comparing this with the average over the whole vehicle (or train). The combined effective roughness is then determined from the rail vertical vibration by applying three conversion spectra [13]. These allow for (i) the difference between the rail head vibration and the vibration at the chosen accelerometer position, which was under the rail foot, (ii) the difference between the effective roughness and the rail head vibration, which depends on the wheel mobility and the contact stiffness, and (iii) the difference between the average rail vibration over the measured length and that at the contact point. The third term depends on the track decay rate which has already been determined as above. Further details are given in [13].

Having determined the combined effective roughness, the total transfer function from roughness to sound pressure can be determined for each test run. This transfer function is a speed-independent quantity, which can be used for predicting the rolling noise at any speed when combined with the effective roughness. The roughness on the other hand depends on wavelength rather than frequency. The analysis was applied to each test run using the vertical rail acceleration at track section A and a microphone at the centre of the beamforming array. The results were averaged over different speeds to obtain the full frequency range. Next, the average roughness levels and average transfer functions were used to reconstruct pass-by levels at each speed over the entire frequency range.

The combined roughness spectrum derived from the PBA method is shown in Figure 14 together with results from the direct measurements (Figure 6) after applying a contact filter. For this purpose two different contact filters were applied: the Remington analytical formula [6, 1], with an assumed contact patch radius of 5.7 mm, and the 'distributed point-reacting springs' (DPRS) model [35, 36], which was also used in determining the reference results. The indirectly measured combined roughness levels match well with the directly measured ones after application of the contact filter.

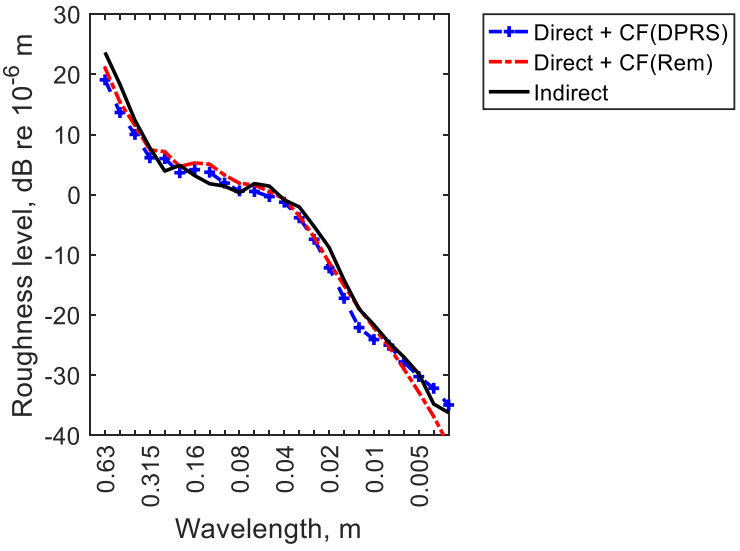

Figure 14. Comparison of direct and indirect measurements of total roughness.

The PBA method was also applied to the passage of service trains as well as the test train. If the total transfer function $L_{HpR,\mathrm{tot}}(f)$ from roughness to noise is measured for the passage of a quiet vehicle (for example one with small or well-damped wheels), then it should be similar

to that of the track alone $L_{HpR,\mathrm{tr}}(f)$. The same is true for the sound pressure level, $L_{p,\mathrm{tot}} \approx L_{p,\mathrm{tr}}$. Other trains passing at the same site were therefore examined to see whether such vehicles were present. It was found that most trains, such as high speed, Intercity and freight trains, had standard wheel sizes, which were therefore not quiet, but one of the two freight trains passing during the test period contained a single 6-axle articulated wagon with 760 mm diameter wheels. However, this was found to have a transfer function spectrum that was only 2 dB lower than the test train in the frequency range above 1 kHz. This was partly due to the fact that the track had a relatively high noise contribution as it has soft rail pads, and consequently a very low track decay rate, as seen in Figure 5. Thus the 'reference vehicle method' could not be applied in the current tests.

Separation could also be achieved if the vehicle transfer function $L_{HpR,\mathrm{veh}}(f)$ is measured using static tests. However, this was not determined as part of the current test programme. By inspection of a previously measured wheel transfer function of a 920 mm wheel it was identified that the crossover frequency between wheel and track noise dominance is likely to occur at around 2 kHz. This information was used to derive track and vehicle contributions using a simple distribution function method. For frequencies below 2 kHz it was assumed that the track is dominant, and the wheel transfer function was assumed to be a notional 7 dB lower than the total transfer function. The track transfer function was set to 1 dB below the total. For frequencies of 2 kHz and above, the wheel transfer function was assumed to be dominant, and the track transfer function was assumed to be 7 dB below the total. Figure 15(a) shows the resulting transfer functions of wheels and track. By adding the combined roughness levels obtained for each train speed, see Figure 14, to the separate transfer functions, the relative contribution of the wheel and the track to the overall pass-by level could be estimated.

As an alternative, a previous static wheel transfer function measurement of a 730 mm diameter reference vehicle from the STAIRRS project [37] was used to estimate the wheel and track transfer functions, see Figure 15(b). The wheel transfer function was estimated from the STAIRRS reference vehicle by shifting the function to lower frequencies by two one-third octave bands to approximate a larger wheel. The track transfer function at higher frequencies was extrapolated by a simple function, so the wheel dominates the noise radiation at higher frequencies.

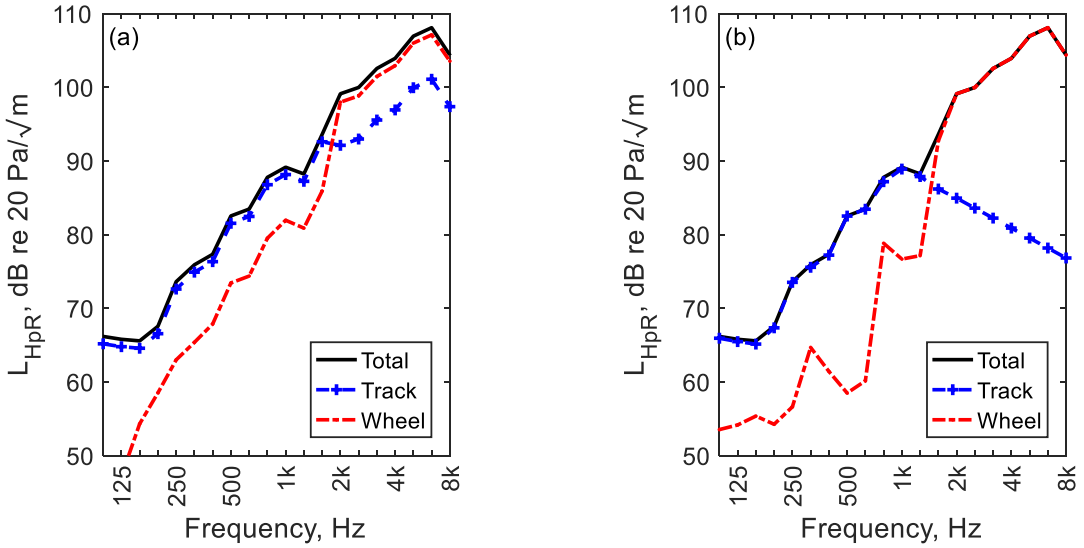

Figure 15. Vehicle and track transfer functions (a) based on assumed distribution function; (b) based on adjusted vehicle transfer function from STAIRRS project.

6. Results

6.1. Reference results

The reference results (as described in Section 4) obtained for track section A are shown in Figure 16(a). These are shown in the form of the level difference between the estimated components (wheel or track) and the measured total noise. Results are shown for three speeds, each being the energy average of three train pass-bys. It can be seen that the results are fairly consistent across the different speeds, with the wheel component being dominant at 2 kHz and above, and the track component being dominant below this. The corresponding results for the three different track sections are shown in Figure 16(b) for a speed of 80 km/h. Again these results are very consistent despite the differences in microphone position.

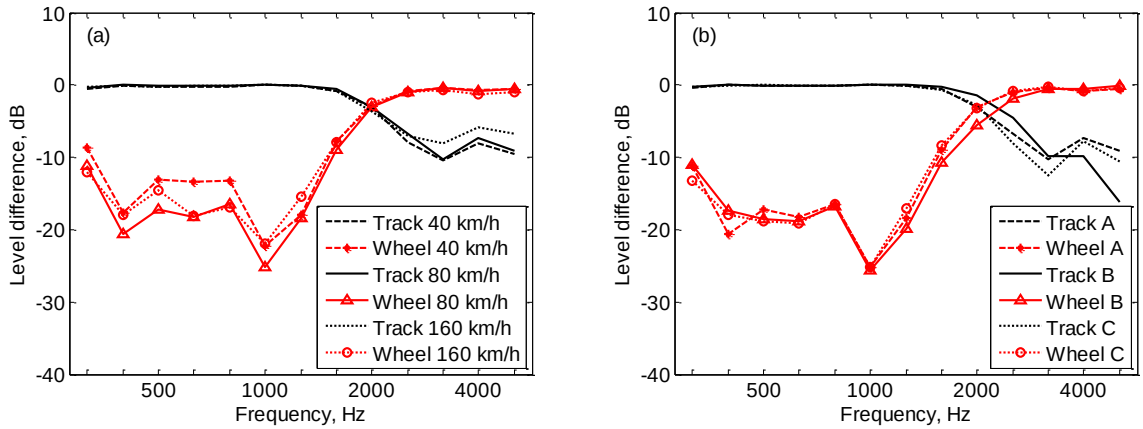

Figure 16. Reference results (a) for track section A at all speeds; (b) for all three track sections at 80 km/h.

6.2. Identification of track component

The track component of noise can be estimated from six different methods described above. Results for four of them are shown in Figure 17 (the others are discussed below). This again shows the level difference between the estimated track component of noise and the measured sound pressure level. In each case the corresponding reference results are also shown. The average results for each speed are shown in each graph.

The estimates obtained from the TWINS model with measured track vibration in Figure 17(a) are, of course, similar to the reference results. The difference lies in the correction applied to the reference results to ensure that the total estimated noise spectrum matches the measured noise spectrum, as shown in Figure 8. This correction has not been applied to the results from the method based on the TWINS model with measured track vibration (Section 5.3) discussed here.

As explained in Section 5.1, the results from the WSE method could only be obtained up to 2 kHz due to the microphone spacing used. The corresponding reference results have therefore not been corrected to the measured spectrum above 2 kHz. The results, shown in Figure 17(b), agree reasonably well, although the WSE results drop below the reference results by up to 3 dB at frequencies above 1.25 kHz and, in one case, below 500 Hz. As mentioned in [29], the differences above 1.25 kHz are attributed to higher-order waves that are not accounted for in the pass band of the wavenumber filters. Although not shown here, it has been investigated in

[34] that using low-pass instead of band-pass filters can reduce the differences above 1.25 kHz.

As shown in Figure 17(c), the ATPA method (Section 5.4) gives results that agree well with the reference results, especially below 1.6 kHz. Above 2.5 kHz the estimate from the ATPA method is somewhat higher than the reference results. However, this may be due to the fact that cross-section deformation of the rail is neglected in the TWINS prediction, whereas no such assumptions are included in the ATPA method.

As shown in Figure 17(d), the MISO method (Section 5.5) underestimates the track component below 2 kHz by 1-2 dB and overestimates it by 5-10 dB at 3.15 kHz and above. The high frequency results are overestimated even when compared with the results from the ATPA method. This may be caused by contamination of the measured track transfer function with noise from the wheels, due to the fact that the microphone was further away from the rail than desirable.

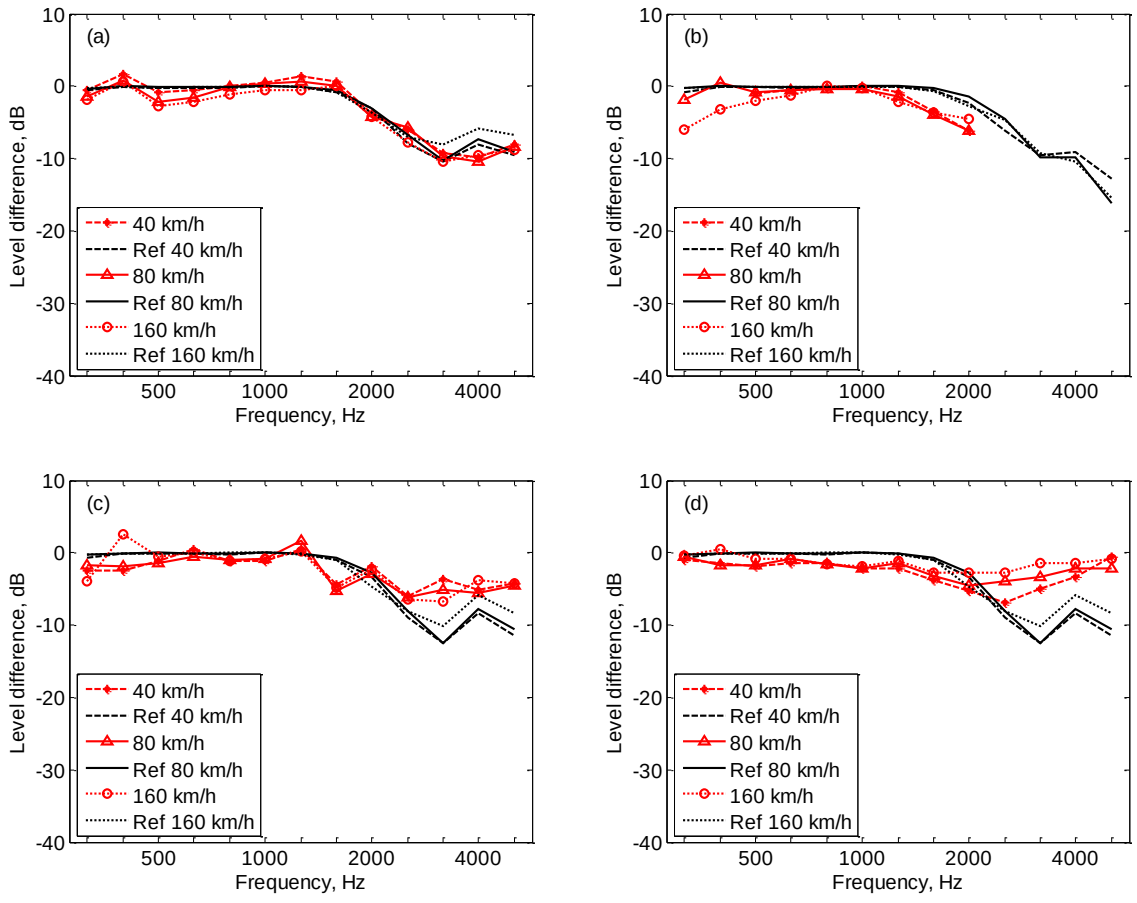

Figure 17. Track component obtained from various methods for all three speeds: (a) TWINS with track vibration; (b) WSE method; (c) ATPA method; (d) MISO method.

Figure 18(a) compares the results from the TWINS radiation models with measured track vibration (see also Figure 17(a)) with the results from the two PBA-based methods for a train speed of 80 km/h; these are all for track section A. The one labelled PBA1 is based on the assumed distribution function plotted in Figure 15(a), i.e. 1 dB below the total for frequencies up to and including 1.6 kHz and 7 dB below the total above this. It can be seen that the chosen cut-off frequency in Figure 15(a) agrees reasonably well with the reference results but the level difference should drop more gradually above 2 kHz. The method labelled PBA2 is based on an earlier wheel transfer function as shown in Figure 15(b). Here, the track transfer function was chosen arbitrarily above 1.6 kHz and can be seen to fall much too rapidly with increasing frequency above this. With hindsight, a different distribution function would have been more appropriate. The results from the three other methods, already shown in Figure 17, are compared for a speed of 80 km/h in Figure 18(b).

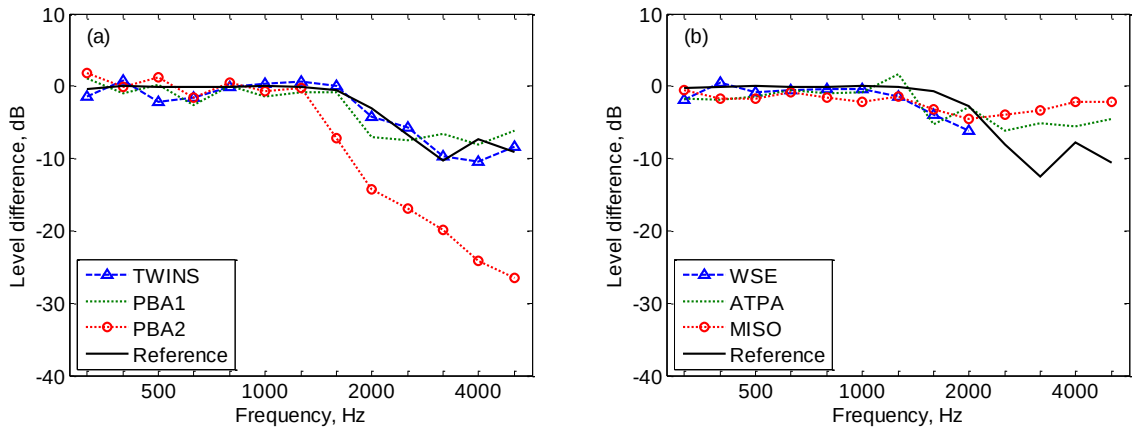

Figure 18. Track component obtained from different methods, 80 km/h. (a) TWINS with measured track vibration and two variants of PBA, including reference results for section A; (b) WSE, ATPA and MISO methods including reference results for section C.

6.3. Identification of wheel component

The only methods capable of identifying the wheel component are the beamforming method and the two PBA-based methods. Results for the beamforming method are shown in Figure 19(a). As before, this shows the level difference between the estimated wheel component of

noise and the measured sound pressure level. In each case the corresponding reference results are also shown. The average results for each speed are shown in each graph. Compared with the reference results it is clear that the beamforming method has not been able to suppress the rail noise contribution as intended; the estimate is close to 0 dB for all frequencies. The results below 1600 Hz appear to be strongly influenced by the rail noise and differ from the reference results for the wheel by more than 10 dB. This could be expected from inspection of the beamforming maps in Figure 12, from which it can be seen that the region away from the bogies still produces noticeable output even when the method was intended to suppress this. The reason for this discrepancy is not known.

The wheel noise estimates from the two PBA-based methods are shown in Figure 19(b). From this it is clear that the nominal distribution function (PBA1) significantly overestimates the wheel contribution below 1.6 kHz. The adapted wheel transfer function (PBA2) appears to be slightly inconsistent with the reference results, dropping at a lower cut-off frequency.

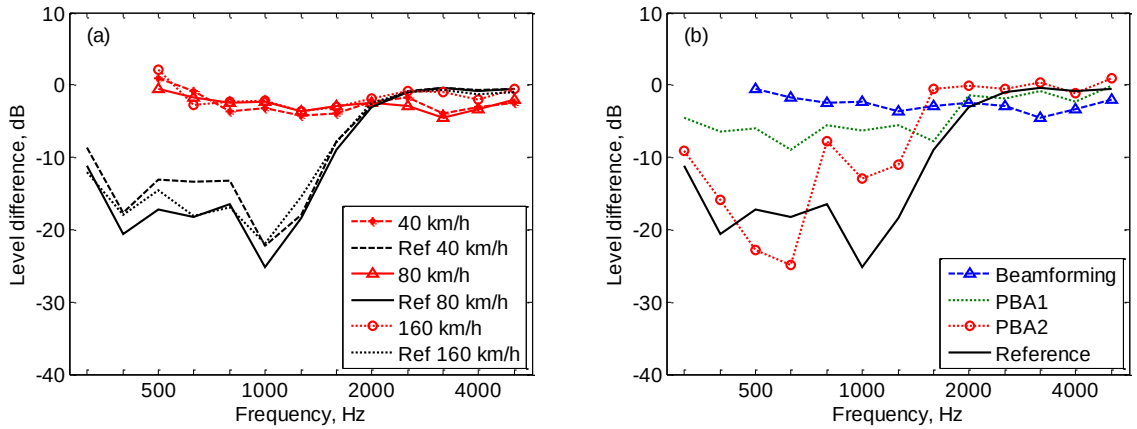

Figure 19. Wheel component: (a) obtained from beamforming method for different speeds; (b) obtained from different methods at 80 km/h.

6.4. Assessment of overall A-weighted levels

The results of the various separation methods are summarised in terms of their A-weighted levels in Tables 3 and 4. Table 3 lists the differences in overall A-weighted levels between the respective estimation methods and the reference results for the track component, and Table 4 gives the corresponding results for the wheel component. Negative values indicate that the estimate is lower than the reference result. All the methods can estimate the track

noise to within 2 dB; the TWINS-based method, ATPA and the PBA method based on the nominal distribution function achieve agreement within 1 dB. The results for the wheel component, however, are much less satisfactory with overestimates of 2-3 dB for both PBA-based methods and of 2-5 dB for the beamforming method, as would be expected from the spectral results seen earlier.

Table 3. Summary of differences in A-weighted track noise level obtained using different methods relative to reference result

	TWINS	PBA1	PBA2	WSE*	ATPA	MISO
40 km/h	0.5	–0.4	–1.0	–1.8	–0.2	–1.3
80 km/h	–0.2	–0.6	–0.5	–0.8	–0.6	–1.2
160 km/h	0.5	–1.0	–1.9	–1.3	–0.3	–0.1

*: based on 315-2000 Hz

Table 4. Summary of differences in A-weighted wheel noise level obtained using different methods relative to reference result

	Beamforming	PBA1	PBA2
40 km/h	2.3	1.8	2.6
80 km/h	4.8	3.0	2.9
160 km/h	3.1	1.7	2.9

6.5 Effect of the presence of the vehicle in the static tests

In the ATPA method, the DTFs were obtained with the vehicle present on the track section. An additional set of measurements was made without the train present. Figure 20 shows the difference between the estimate of track noise obtained using the DTFs without the vehicle and those obtained with the vehicle in place. If the presence of the vehicle is not taken into account, the track component is found to be on average 2.1 dB lower than when using the DTFs measured with the vehicle in place. The results are very consistent over different speeds. The standard deviation over frequency bands is 1.8 dB. This difference is expected to be mainly due to the change in directivity associated with reflections from the underside of the train. In the TWINS model this is taken into account approximately by using a directivity

for the rail vertical component that is omnidirectional rather than a vertical dipole which is more appropriate for a free rail [1].

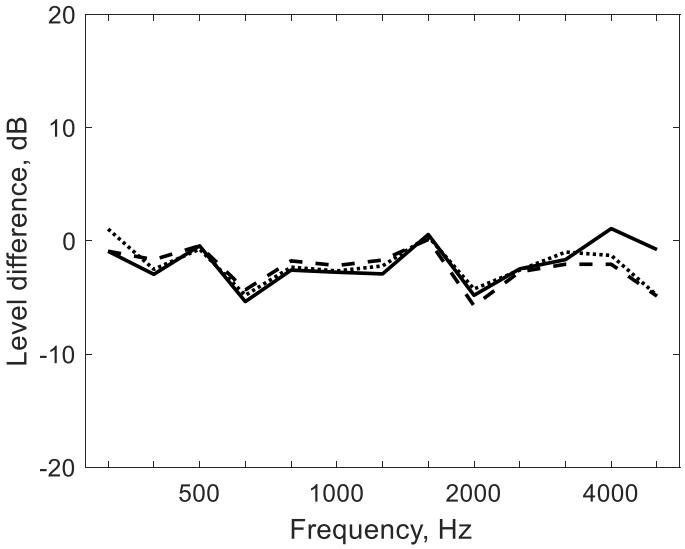

Figure 20. Level difference between the estimate of track noise obtained using the DTFs without the vehicle and those obtained with the vehicle in place. - - - 40 km/h, — 80 km/h, ····· 160 km/h.

7. Conclusions

Field tests have been carried out under controlled conditions to allow assessment of several existing and new methods for rolling noise separation. The TWINS model has been used with measured vibration data to give reference estimates of the wheel and rail source contributions. Six different methods were then considered that can be used to estimate the track component of noise. It was found that most of these methods could obtain the track component with acceptable accuracy, giving A-weighted levels within 1-2 dB of the reference results. The wave signature extraction method was only tested up to 2 kHz and gave a small underestimate of the track noise above 1250 Hz. In principle the 2 kHz limit can be increased by means of using a denser array, and the estimation above 1.25 kHz is expected to improve if low-pass instead of band-pass wavenumber filters are used. The MISO method is particularly simple to implement but gave underestimates of the track noise below 2 kHz and overestimates of 5-10 dB at high frequencies. It is expected that this could be improved by using a microphone closer to the track. The ATPA method is more complex to implement, requiring access to the track for the measurement of transfer functions, but it gave very good

results. It suggests that the track noise is slightly higher at high frequency than the TWINS model indicates, which is likely to be due to the neglect of rail cross-section deformation in the TWINS model.

Apart from the TWINS model, the wheel noise component could only be estimated directly using three of the methods, the beamforming method and two based on the Pass-by Analysis method, but unfortunately these did not give satisfactory results in the current tests. The PBA results could be improved by taking static measurements of the wheel transfer function. The estimates of the track noise from these methods were more reasonable than those of the wheel.

For implementation in a practical situation, for example as part of standard vehicle testing procedures, the cost and practicality of the methods would also need to be considered. Some discussion of this is given in reference [34]. The work carried out is not yet directly applicable for certification testing. Further development for measuring wheel transfer functions including possible hybrid methods, further validation and standardization as well as application of transposition methods from one track to another is necessary.

Acknowledgements

The work described in this paper has been carried out as part of the Roll2Rail project, which has been financially supported by the European Union's Horizon 2020 grant, agreement No. 636032. The authors are grateful to the staff of Deutsche Bahn without whom the field tests would not have been possible, to the many colleagues who assisted in the tests and for the leadership of former colleagues Siv Leth, Adam Mirza and Ulf Orrenius. All data published in this paper are openly available from the University of Southampton repository at https://doi.org/10.5258/SOTON/D0520.

References

[1] D. Thompson, Railway Noise and Vibration: Mechanisms, Modelling and Means of Control, 1st ed. Elsevier, 2009.

[2] P.E. Gautier, F. Poisson and F. Letourneaux, High speed trains external noise: a review of measurements and source models for the TGV case up to 360 km/h. Proceedings of World Congress on Railway Research, Seoul, 2008.

[3] Commission Regulation (EU) No 1304/2014 of 26 November 2014 on the technical specification for interoperability relating to the subsystem ‘rolling stock — noise’, Official Journal of the European Union, L356/421-437, 2014.

[4] ISO 3095:2013. Acoustics – Railway applications – Measurement of noise emitted by railbound vehicles, International Standards Organization, Geneva, 2013.

[5] P.J. Remington. Wheel/rail rolling noise, I: Theoretical analysis, Journal of the Acoustical Society of America 81, 1805-1823, 1987.

[6] P.J. Remington. Wheel/rail noise, part IV: rolling noise. Journal of Sound and Vibration 46, 419-436, 1975.

[7] D.J. Thompson. Theoretical modelling of wheel-rail noise generation, Proceedings of the Institution of Mechanical Engineers, Journal of Rail and Rapid Transit, 205F, 137-149, 1991.

[8] D.J. Thompson, B. Hemsworth, N. Vincent, Experimental validation of the TWINS prediction program, part 1: method. Journal of Sound and Vibration 191, 123-135, 1996.

[9] D.J. Thompson, P. Fodiman, H. Mahé, Experimental validation of the TWINS prediction program, part 2: results. Journal of Sound and Vibration 193, 137-147, 1996.

[10] C.J.C. Jones, D.J. Thompson, Extended validation of a theoretical model for railway rolling noise using novel wheel and track designs. Journal of Sound and Vibration 267, 509-522, 2003.

[11] S.L. Grassie, M. Saxon and J.D. Smith, 1999 Measurement of longitudinal rail irregularities and criteria for acceptable grinding. Journal of Sound and Vibration 227(5), 949-964.

[12] G. Squicciarini, M.G.R. Toward, C.J.C. Jones, D.J. Thompson, 2015, Statistical description of wheel roughness, In J.C.O. Nielsen et al. (eds.), Noise and Vibration Mitigation for Rail Transportation Systems, Notes on Numerical Fluid Mechanics & Multidisciplinary Design 126, 651-658.

[13] M.H.A. Janssens, M.G. Dittrich, F.G. de Beer, C.J.C. Jones, Railway noise measurement method for pass-by noise, total effective roughness, transfer functions and track spatial decay, Journal of Sound and Vibration 293 (2006) 1007–1028.

[14] M.G. Dittrich, F. Létourneaux, H. Dupuis, Background for a new standard on pass-by measurement of combined roughness, track decay rate and vibro-acoustic transfer functions, In J.C.O. Nielsen et al. (eds.), Noise and Vibration Mitigation for Rail

Transportation Systems, Notes on Numerical Fluid Mechanics & Multidisciplinary Design 126, 197-204.

[15] CEN/TR 16891:2016. Railway applications – Acoustics – Measurement method for combined roughness, track decay rates and transfer functions. Technical Report, European Committee for Standardization, Brussels, 2016.

[16] F. G. de Beer, J. W. Verheij, Experimental determination of pass-by noise contributions from the bogies and superstructure of a freight wagon, Journal of Sound and Vibration 231(3), 639-652, 2000.

[17] F. Létourneaux – STAIRRS Report - D11 Part 5 - MISO: A measurement method to separate noise emission of railway vehicles and tracks, November 2003

[18] M. Wirnsberger, M.G. Dittrich et al, The METARAIL Project - Final Report, Project no. RA-97-SC.1080, Metarail Consortium, 1999.

[19] M.G. Dittrich, M.H.A. Janssens, Improved measurement methods for railway rolling noise, Journal of Sound and Vibration (2000) 231(3), 595-609.

[20] J.J. Christensen, J. Hald, Beamforming, Brüel & Kjaer Technical Review, No. 1, 2004.

[21] B. Barsikow, W.F. King III and E. Pfizenmaier, Wheel/rail noise generated by a high speed train investigated by a line array of microphones, Journal of Sound and Vibration 118, 99-122, 1987.

[22] C. Talotte, Aerodynamic noise, a critical survey. Journal of Sound and Vibration 231, 549-562, 2000.

[23] B. Barsikow and W.F. King III, On removing the Doppler frequency shift from array measurements of railway noise. Journal of Sound and Vibration 120, 190-196, 1988.

[24] B. Barsikow, Experiences with various configurations of microphone arrays used to locate sound sources on railway trains operated by the DB AG. Journal of Sound and Vibration 193, 283-293, 1996.

[25] A. Nordborg, A. Martens, J. Wedermann, L. Willenbrink, Wheel/rail noise separation with microphone array measurements, Internoise 2001, The Hague, August 2001.

[26] T. Kitagawa, D.J. Thompson. The horizontal directivity of noise radiated by a rail and implications for the use of microphone arrays. Journal of Sound and Vibration 329(2), 202-220, 2010.

[27] EN 15461:2008. Railway applications – Noise emissions, Characterization of the dynamic properties of track sections for pass by noise measurements, European Committee for Standardization, Brussels, 2008.

[28] E. Zea, L. Manzari, I. Lopez Arteaga, G. Squicciarini, D. Thompson. Separation of track contribution to pass-by noise by near-field array techniques. Proceedings of the 22nd International Congress on Acoustics, Buenos Aires, 2016.

[29] E. Zea, L. Manzari, G. Squicciarini, L. Feng, D. Thompson, I. Lopez Arteaga. Wavenumber–domain separation of rail contribution to pass-by noise. Journal of Sound and Vibration 409, 24-42, 2017.

[30] B. Faure, O. Chiello, M.-A. Pallas, C. Servière. Characterisation of the acoustic field radiated by a rail with a microphone array: The SWEAM method. Journal of Sound and Vibration 346, 165-190, 2015.

[31] J. Zhang, G. Squicciarini and D. Thompson, Beamforming approaches for railway noise source identification, First International Conference on Rail Transportation, July 2017, Chengdu, China.

[32] F.X. Magrans, Method of measuring transmission path, Journal of Sound and Vibration, 74(3), 321-330, 1981.

[33] A. Malkoun, J. Sapena, K. Arcas, F.X. Magrans. Vehicle and rail noise separation method proposal based on transfer path analysis techniques. 21st International Congress on Sound and Vibration, Beijing, 2014.

[34] D. Thompson, G. Squicciarini, J. Wändell, I. Lopez Arteaga, E. Zea Marcano, A. Malkoun, E. Iturritxa, A. Guiral, I. Gutiérrez, G. Schleinzer, M. Stangl, B. Martin Lopez, C. Chaufour, Roll2Rail Deliverable D7.4 – Assessment and validation of source separation methods, April 2017.

[35] P. Remington, J. Webb. Estimation of wheel/rail interaction forces in the contact area due to roughness. Journal of Sound and Vibration 193, 83-102, 1996.

[36] D.J. Thompson. The influence of the contact zone on the excitation of wheel/rail noise. Journal of Sound and Vibration 267, 523-535, 2003.

[37] H.W. Jansen, F.G. de Beer, M.G. Dittrich: Validation measurements for level 2 measurements with indirect roughness, TNO report DGT-RPT-020078, STAIRRS deliverable, report STR23TR150702TNO2, July 2002.